

# Angle-resolved photoion yield and resonant Auger spectroscopy for the doubly excited Rydberg states above the C 1s threshold of CO

M. Kitajima,<sup>1,\*</sup> R. Püttner,<sup>2,3</sup> S. L. Sorensen,<sup>4</sup> T. Tanaka,<sup>1</sup> M. Hoshino,<sup>1</sup> H. Fukuzawa,<sup>2</sup> A. De Fanis,<sup>5</sup> Y. Tamenori,<sup>5</sup> R. Sankari,<sup>6</sup> M. N. Piancastelli,<sup>7</sup> H. Tanaka,<sup>1</sup> and K. Ueda<sup>2,†</sup>

<sup>1</sup>Department of Physics, Sophia University, Tokyo 102-8554, Japan

<sup>2</sup>Institute of Multidisciplinary Research for Advanced Materials, Tohoku University, Sendai 980-8577, Japan

<sup>3</sup>Institut für Experimentalphysik, Freie Universität Berlin, D-14195 Berlin-Dahlem, Germany

<sup>4</sup>Department of Synchrotron Radiation Research, Institute of Physics, University of Lund, Box 118, SE 221 00 Lund, Sweden

<sup>5</sup>Japan Synchrotron Radiation Research Institute, Sayo-gun, Hyogo 679-5198, Japan

<sup>6</sup>Department of Physics, Materials Science, University of Turku, FI-20014 Turku, Finland

<sup>7</sup>Department of Physics, Uppsala University, Box 530, SE-751 21 Uppsala, Sweden

(Received 14 May 2008; published 19 September 2008)

Doubly excited core-hole states of carbon monoxide in the photon energy region of 300–305 eV, i.e., directly above the C 1s ionization threshold, have been studied using both angle-resolved ion-yield and high-resolution resonant Auger spectroscopies. The leading configurations of the most prominent doubly excited Rydberg states are assigned by careful analysis of the ion-yield spectra and the final-state spectra to C  $1s^{-1} (5\sigma^{-1}2\pi^1 S=1) 3s\sigma (v'=0,1,2)$ , C  $1s^{-1} (5\sigma^{-1}2\pi^1 S=0) 3s\sigma (v'=0,1,2)$ , and C  $1s^{-1} (5\sigma^{-1}2\pi^1 S=1) 4s\sigma (v'=0,1)$ , which can only be populated via a conjugate shake-up process. Analysis of the resonant Auger spectra provides an assignment of several two-hole–one-electron ( $2h-1e$ ) final states.

DOI: [10.1103/PhysRevA.78.033422](https://doi.org/10.1103/PhysRevA.78.033422)

PACS number(s): 33.80.Eh, 33.20.-t

## I. INTRODUCTION

Carbon monoxide is one of the showcases of core-level spectroscopy and has provided a number of important insights into the electronic structure of core-excited diatomic molecules. The carbon  $K$ -shell ion-yield spectrum exhibits well-resolved features arising from core to Rydberg excited states below the carbon  $K$  edge [1,2] while above threshold both broad resonant features and narrow well-defined peaks have been identified in many experiments [2–10]. The broad feature at  $\cong 305$  eV has been assigned to the  $\sigma^*$  shape resonance, while the sharp features at slightly lower energy are attributed to vibrational progressions of doubly excited Rydberg states converging to satellite states of the C 1s ionization threshold. Ågren and Arneberg identified these as shake-up transitions associated with C  $1s \rightarrow 2\pi$  excitation by theoretical treatment [11]. They were first measured by Shaw *et al.* using electron-energy loss spectroscopy [4], and later by Domke *et al.* [2], Ma *et al.* [5], and Köppe *et al.* [9] using ion-yield spectroscopy. Köppe *et al.* [9] also measured photoelectron spectra of C  $1s^{-1}$  main line at the photon energy around the doubly excited Rydberg states. Based on these extensive studies there is a general agreement that the configurations are most likely given by a C  $1s \rightarrow 2\pi$  excitation accompanied by a shake up from the  $1\pi$  or  $5\sigma$  orbital to a  $n\ell\lambda$  Rydberg orbital. The precise configurations of these states have not been determined.

Resonant Auger spectroscopy is a powerful tool for the study of inner-valence spectra of atoms and molecules by measuring the projection of the core-excited state onto the

final states [12–14]. The core-excited states and the final states are often related to each other by the strict spectator model, i.e., by assuming that the excited electron remains in its orbital during the Auger decay. By applying this model one expects that the final states with an excited electron in the particular orbital are resonantly enhanced. This method relies on an understanding of the involved intermediate core-excited states; for studies where the final states are known, the spectra reveal the details of the core-excited state. As an example, Öhrwall *et al.* compared the resonant Auger spectra of C  $1s \rightarrow ns, np$  Rydberg excitations to high-resolution inner-valence spectra [15]. Despite the relatively low resolution of the resonant Auger spectra many features in the high-resolution inner-valence spectrum could be identified.

The decay pathways of doubly excited core-hole states can be classified into several types as discussed by Schmidbauer *et al.* [16]. As these states lie in the core-ionization continuum, they can autoionize into the singly ionized core-hole states, which subsequently decay by the normal Auger process. The Bradshaw group showed that autoionization of doubly excited Rydberg states leads to a substantial vibrational enhancement in carbon  $K$ -shell ionization in CO [8,9,17]. The measured vibrational branching ratios were reproduced in a simulation employing a harmonic potential [9].

In addition, three different types of radiationless decay channels are possible for the core hole: participator Auger decay, in which both of the excited electrons participate in the Auger decay leads to singly ionized final states with 1 hole in the valence shell and no excited electrons, i.e., a  $1h-0e$  state. Single spectator Auger decay, in which one of the excited electrons remains as a spectator electron in its orbital during the decay, results in a final state with two holes in the valence shell, and one excited electron, i.e., they are  $2h-1e$  states. These states are also accessible via spectator Auger decay of core-excited states. The third decay path is

\*Present address: Department of Chemistry, Tokyo Institute of Technology, Tokyo 152-8551, Japan.

†ueda@tagen.tohoku.ac.jp

double spectator decay, i.e., both excited electrons remain as spectator electrons in their orbitals. The final state has a  $3h-2e$  configuration.

Auger spectra following C  $1s$  photoexcitation in CO have been presented in many studies [15,18–23]. In contrast, very few studies on resonant Auger from the doubly excited Rydberg states have been reported. The only photon energy dependent resonant Auger spectra in the region of the doubly excited Rydberg states is by Schmidbauer *et al.* [17]. The spectra showed distinct resonance-dependent features at about 33 eV binding energy, but the limited resolution of this study (1.5 eV) prevented a deeper analysis of the origin of these features. Hemmers *et al.* also recorded resonant Auger spectra at the photon energy including 300.9 eV, where the doubly excited Rydberg states lie [22]. However, their attention was focused on the resonant Auger spectra from the singly excited Rydberg states.

Angle-resolved ion-yield spectra allow the total symmetry of the doubly excited states to be determined. In this study we measure resonant Auger spectra at the energies of the discrete features around 300 eV in order to understand the intermediate states, and to make an assignment of these states. Several  $2h-1e$  states in the resonant Auger spectra are assigned, and the origin of their resonant behavior is discussed. We are thus able to assign a number of states in the inner-valence photoelectron spectra.

## II. EXPERIMENT

The experiments have been carried out using the  $c$  branch of the soft x-ray photochemistry beam line 27SU [24] at the SPring-8 synchrotron radiation facility in Japan. This beam line is equipped with a high-resolution Hettrick-type monochromator with a varied line-spacing plane grating [25,26].

The Auger spectra were recorded with a Gammadata-Scientia SES2002 electron spectrometer equipped with a gas cell [27,28]. This spectrometer accepts electrons emitted along the horizontal axis of the plane perpendicular to the propagation direction of the beam. The source is a figure-8 undulator that provides linearly polarized light with a horizontal (first-order harmonic) or vertical (0.5th-order harmonic) polarization vector [29]. By selecting the direction of the electric field vector of the incident light, electron spectra for  $\theta=0^\circ$  and  $90^\circ$  can be obtained without rotating the spectrometer. Here,  $\theta$  is the angle between the emitted electron and electric vector of the incident light.

The photon bandwidth of the monochromator was set to  $\approx 66$  meV full width at half maximum (FWHM) at 300 eV. The electron analyzer was used at constant pass energy of 100 eV and a slit width of 0.2 mm. These values result in an electron-energy bandwidth of  $\approx 66$  meV FWHM. The Doppler width due to the thermal motion of target CO molecule was estimated to be about  $\approx 38$  meV resulting in an overall resolution of  $\approx 100$  meV.

Symmetry-resolved ion-yield spectra were measured using two identical retarding-potential type ion detectors [30]. The applied retarding potential was 6 V. The detectors were mounted along the horizontal and the perpendicular axis of the plane perpendicular to the propagation direction of the

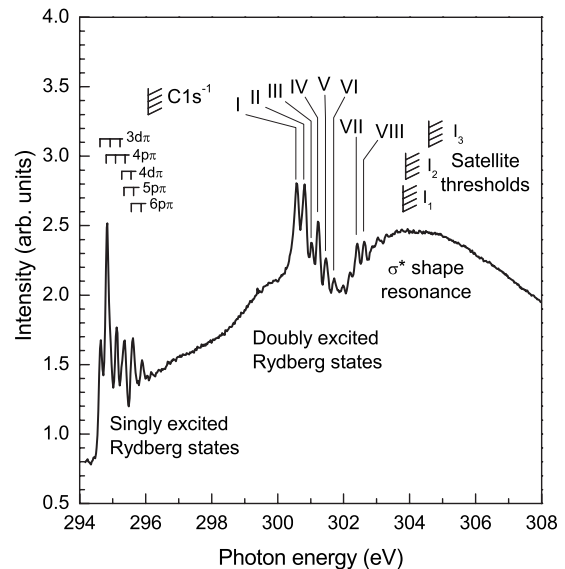


FIG. 1. Total ion-yield spectrum of CO near the C  $1s^{-1}$  edge. The resonant Auger spectra presented in this work were measured at the photon energies of peaks I–VIII.

incident light, i.e., they detect fragment ions emitted parallel or perpendicular to the polarization direction of the light; thus for a diatomic molecule these correspond to transitions of  $\Sigma$  and  $\Pi$  symmetries. The symmetry-resolved ion-yield measurements were performed at a photon energy resolution of 66 meV and the energy scale was calibrated using the values of the doubly excited Rydberg states at 300–303 eV published by Domke *et al.* [2].

Magic angle ( $54.7^\circ$ ) spectra, which are equivalent to the angle integrated spectra can be constructed by combining the  $0^\circ$  and  $90^\circ$  spectra according to the equation

$$I_e(54.7^\circ) = I_e(0^\circ) + 2I_e(90^\circ), \quad (1)$$

where  $I_e(0^\circ)$  and  $I_e(90^\circ)$  are the intensities of the electron or ion-yield spectra measured at those angles.

The photon flux was monitored by the drain current on the last beamline mirror upstream of the experimental setup and by a photodiode current downstream of the experimental setup. However, in the region of the C  $1s$  ionization threshold the measurements of the photon flux by photocurrent suffer from carbon contaminations on the surface of the optical components so that the photon-flux reading was corrected by comparing the intensities of angle-resolved Ar  $2p$  photoelectron spectra with the known cross sections and angular distributions at the photon energy of interest [31,32]. The degree of linear polarization was confirmed to be larger than 0.98. The experiments were performed using commercially obtained carbon monoxide gas with a purity of  $>99.99\%$ .

## III. TOTAL AND SYMMETRY-RESOLVED ION-YIELD SPECTRA

The total ion-yield spectrum of CO across the C  $1s^{-1}$  edge is shown in Fig. 1. In the below-threshold region the spec-

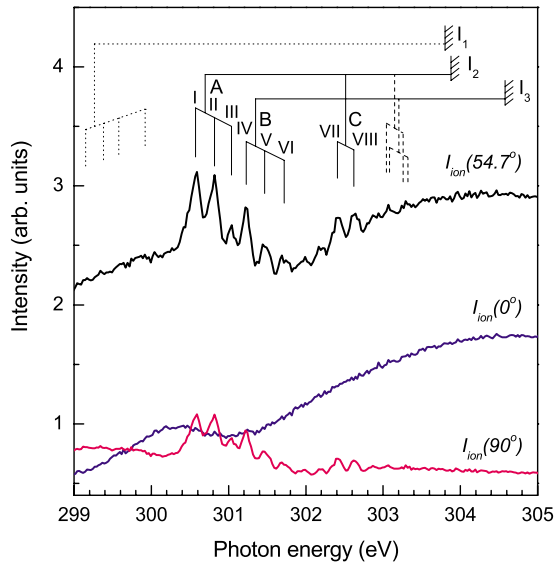


FIG. 2. (Color online) The symmetry-resolved C  $1s$  near-edge ion-yield spectrum. The spectral components corresponding to perpendicular transitions [ $I_{ion}(90^\circ)$ ], i.e., with final states of  $\Pi$  symmetry, and parallel transitions [ $I_{ion}(0^\circ)$ ], i.e., with final states of  $\Sigma$  symmetry are shown. The [ $I_{ion}(54.7^\circ)$ ] curve represents the angle-integrated absorption spectrum.

trum shows the well-known C  $1s \rightarrow n\ell\lambda$  states [1,2]. Above the C  $1s^{-1}$  threshold, the broad  $\sigma^*$  shape resonance can be seen around 305 eV, together with a number of sharp peaks around 300 eV. According to Domke *et al.* [2] these peaks can be assigned to three different transitions: peaks I–III are the vibrational substates of the transition A, peaks IV–VI are the vibrational substates of transition B, and peaks VII and VIII to substates of transition C as shown in Fig. 2.

Domke *et al.* carried out a Franck-Condon analysis of the vibrational substates for states A and B and found equilibrium distances of  $r_e = 1.197 \text{ \AA}$  and  $r_e = 1.174 \text{ \AA}$ , respectively [2]. These values indicate a substantial bond lengthening with respect to both the ground state and to the below-threshold core-excited Rydberg states.

In Fig. 1 the low-lying satellites of the C  $1s$  threshold are labeled as  $I_1$ – $I_3$ . These thresholds are the most probable limits for the doubly excited Rydberg states. Using symmetry-resolved photoelectron spectra and *ab initio* calculations [33]  $I_1$  was assigned to be of  $\Sigma$  symmetry and  $I_2$  and  $I_3$  of  $\Pi$  symmetry. The following discussion is based on the notation  $1\sigma^2 2\sigma^2 3\sigma^2 4\sigma^2 1\pi^4 5\sigma^2 2\pi^0$  for the electronic ground state of neutral CO, where  $1\sigma$  and  $2\sigma$  denote the O  $1s$  and C  $1s$  core orbitals. The configuration of  $I_1$  is C  $1s^{-1} (1\pi^{-1} 2\pi S=1) ^2\Sigma$ . Here  $S$  denotes the total spin formed by the two open valence shells  $1\pi$  and  $2\pi$  with  $S=1$  indicating a triplet state. This configuration is predominantly a direct shake-up satellite with a calculated equilibrium distance of  $r_e = 1.292 \text{ \AA}$  and vibrational splittings of less than 200 meV. The thresholds  $I_2$  and  $I_3$  are assigned to the conjugate shake-up satellites C  $1s^{-1} (5\sigma^{-1} 2\pi S=1) ^2\Pi$  and C  $1s^{-1} (5\sigma^{-1} 2\pi S=0) ^2\Pi$ , i.e., the splitting is due to the two possible relative spin orientations of the hole in the  $5\sigma$  orbital and the electron in the  $1\pi$  orbital. For  $I_2$  the two lowest vibrational spacings in the photoelectron spectrum are  $\cong 240 \text{ meV}$  and  $\cong 220 \text{ meV}$  and for

$I_3$  they are  $\cong 230 \text{ meV}$  and  $\cong 220 \text{ meV}$ . The equilibrium distances for the satellite core-ionized states at  $I_2$  and  $I_3$  are calculated to be  $r_e = 1.168$  and  $1.194 \text{ \AA}$  [33]. By assuming that the Rydberg electron weakly affects the bond distance and by comparing the equilibrium distances of the ionization satellites with those of the doubly excited states derived by Domke *et al.* [2] we conclude that the narrow doubly excited states converge to the  $I_2$  and  $I_3$  thresholds of  $\Pi$  symmetry.

The angle-resolved C  $1s$  near-edge ion-yield spectra are presented in Fig. 2. The curve represented by [ $I_{ion}(90^\circ)$ ] shows the spectral components corresponding to perpendicular transitions, i.e., with final states of  $\Pi$  symmetry, and the curve by [ $I_{ion}(0^\circ)$ ] the parallel transitions, i.e., with final states of  $\Sigma$  symmetry. The [ $I_{ion}(54.7^\circ)$ ] curve is constructed from these two measurements according to Eq. (1).

The fine structure of the doubly excited states is clearly seen in the  $90^\circ$  spectrum in Fig. 2, but these features are not visible in the  $0^\circ$  spectrum, indicating a  $\Pi$  symmetry for these states. A broad feature at  $h\nu \cong 299 \text{ eV}$  recently assigned to the dissociative doubly excited state C  $1s^{-1} 1\pi^{-1} 2\pi^2$  [34] is also seen in the  $90^\circ$  spectrum.

Since the Rydberg excitations converge to the thresholds  $I_2$  and  $I_3$  and since they possess a total  $\Pi$  symmetry we immediately conclude that the configuration should be C  $1s^{-1} 5\sigma^{-1} 2\pi^1 n\ell\lambda$  with  $\lambda = \sigma$ . Accordingly, the doubly excited states are due to conjugate shake up with C  $1s \rightarrow 2\pi$  and  $5\sigma \rightarrow n\ell\sigma$ . As a consequence, the total spin of the electrons in the  $2\pi$  and the  $5\sigma$  orbitals are independent of each other and can form either a singlet ( $S=0$ ) or a triplet ( $S=1$ ). On the basis of the resonant Auger spectra (see below) we identify  $\ell=0$ , i.e., we suggest  $n\sigma$  Rydberg states. By applying the Rydberg formula we assign the peaks I–III belonging to state A to vibrational substates  $v'=0,1,2$  of the C  $1s^{-1} (5\sigma^{-1} 2\pi^1 S=1) 3s\sigma$  state, the transition C (peaks VII and VIII) to  $v'=0,1$  of the state C  $1s^{-1} (5\sigma^{-1} 2\pi^1 S=1) 4s\sigma$ , and the transition B (Peaks IV–VI) to the vibrational substates  $v'=0,1,2$  of the state C  $1s^{-1} (5\sigma^{-1} 2\pi^1 S=0) 3s\sigma$ . Note, that  $v'$  indicates the vibrational substates of the core-excited states and  $v''$  the vibrational substates of the final states of the resonant Auger decay. Based on this assignment we can readily explain the weak peaks at higher energy as the  $v'=0,1$  excitations of the C  $1s^{-1} (5\sigma^{-1} 2\pi^1 S=1) 5s\sigma$  state overlapping with the C  $1s^{-1} (5\sigma^{-1} 2\pi^1 S=0) 4s\sigma$  state as indicated with the broken lines in Fig. 2; note that these structures are clearly visible in the spectrum of Domke *et al.* [2].

A strong broad feature caused by the  $\sigma^*$  shape resonance dominates the  $0^\circ$  spectrum in Fig. 2. In addition, a small hump with a width of about 1 eV was observed at  $\cong 300 \text{ eV}$ . Its width is comparable to that of the vibrational envelope for the satellite  $I_1$  in the angle-resolved photoelectron spectrum [33] and its energy is slightly lower than the C  $1s^{-1} (5\sigma^{-1} 2\pi^1 S=1) 3s\sigma$  excitations. Domke *et al.* found a very weak vibrational progression in this region with a splitting that matches the satellite  $I_1$  so we tentatively assign this spectral feature to the state C  $1s^{-1} 1\pi^{-1} 2\pi^1 3s\sigma$ . This final state implies a direct shake-up process with a C  $1s \rightarrow 3s\sigma$  excitation accompanied by a  $1\pi \rightarrow 2\pi$  shake transition.

#### IV. RESONANT AUGER SPECTRA

##### A. Overview and general remarks on the assignments

Resonant Auger spectra measured at peaks I–VIII are shown in Fig. 3 together with the spectrum recorded at 306 eV. The 306-eV spectrum is essentially the direct inner-valence photoelectron spectrum and can be considered to be the nonresonant background of the resonant Auger spectra. The overall shape of this spectrum closely resembles inner-valence photoelectron spectra obtained at photon energies around 45 eV [15,35]. The broad structure observed at binding energies around 38 eV is the  $3\sigma^{-1}2\Sigma^+$  band.

The high-resolution resonant Auger spectra show strong photon-energy-dependent resonant enhancement. In the following we discuss the assignment of the lines in the resonant Auger spectra. This will also confirm our assignment of the doubly excited states. The energy region of the narrow lines in Fig. 3 is identical to that of the resonant Auger study from the C  $1s^{-1}3s\sigma$  and C  $1s^{-1}np\pi$  excitations [18,19,21], i.e., we clearly measure  $2h-1e$  final states. These states can be described in a first approximation by the  $2h$  “parent states” with an additional electron in a Rydberg orbital. Thus we have a spectator resonant Auger decay with the  $2\pi$  electron as the participator and the Rydberg electron as a spectator.

Narrow linewidths indicate that the final state is bound within the Franck-Condon region. In CO the possible quasisable parent states in order of increasing energy are  $X^3\Pi$  (main configuration:  $1\pi^{-1}5\sigma^{-1}$ ),  $a^1\Sigma^+$  ( $5\sigma^{-2}$ ),  $b^1\Pi$  ( $1\pi^{-1}5\sigma^{-1}$ ),  $A^1\Sigma^+$  ( $4\sigma^{-1}5\sigma^{-1}$ ), and  $d^1\Sigma^+$  ( $4\sigma^{-1}5\sigma^{-1}$ ). The energy splittings between the  $X^3\Pi$  state and the  $a^1\Sigma^+$ ,  $b^1\Pi$ ,  $A^1\Sigma^+$ ,  $d^1\Sigma^+$  state are 185, 530, 2540, and 4180 meV, respectively [36,37]; they are indicated by the vertical bar diagram in the uppermost panel of Fig. 3. Note, that the parent state  $X^3\Pi$  is not populated in the Auger decay subsequent to C  $1s$  ionization so we do not expect that it is strongly populated in the resonant Auger decay from the C  $1s^{-1}n\ell\lambda$  state. For the resonant Auger decay of the C  $1s^{-1}5\sigma^{-1}2\pi^1 ns\sigma$  states the situation is, however, different since the hole in the  $5\sigma$  orbital already exists in the core-excited state so that the population of this parent state is only due to an interplay between the  $1\pi$  and  $2\pi$  electrons.

To obtain the  $2h-1e$  states we have to couple, e.g., an additional  $3s\sigma$  Rydberg electron to the parent states. In the single-configuration picture we find  $1\pi^{-1}5\sigma^{-1}({}^3\Pi)3s\sigma$  ( ${}^{4,2}\Pi$ ),  $5\sigma^{-2}({}^1\Sigma^+)3s\sigma$  ( ${}^2\Sigma^+$ ),  $1\pi^{-1}5\sigma^{-1}({}^1\Pi)3s\sigma$  ( ${}^2\Pi$ ),  $4\sigma^{-1}5\sigma^{-1}({}^3\Sigma^+)3s\sigma$  ( ${}^{4,2}\Sigma^+$ ), and  $4\sigma^{-1}5\sigma^{-1}({}^1\Sigma^+)3s\sigma$  ( ${}^2\Sigma^+$ ). Since the Auger decays under investigation start from singlet states we expect that the spectrum is dominated by doublet states, while quartet states can be neglected. Although the  $3s\sigma$  orbital is known to have some valence character in a C  $1s^{-1}3s\sigma$  core excitation and although we expect the same behavior in the final states we assume that the energetic sequence of the final states does not differ markedly from that of the parent states.

In the following discussion we divide the lines into different groups based on their energy positions and their intensity in the different Auger spectra. We first discuss the groups  $a$ – $h$ , which consist of narrow lines, and finally, the broad line  $X$ , which is lowest in energy. The energies of all lines are collected in Table I.

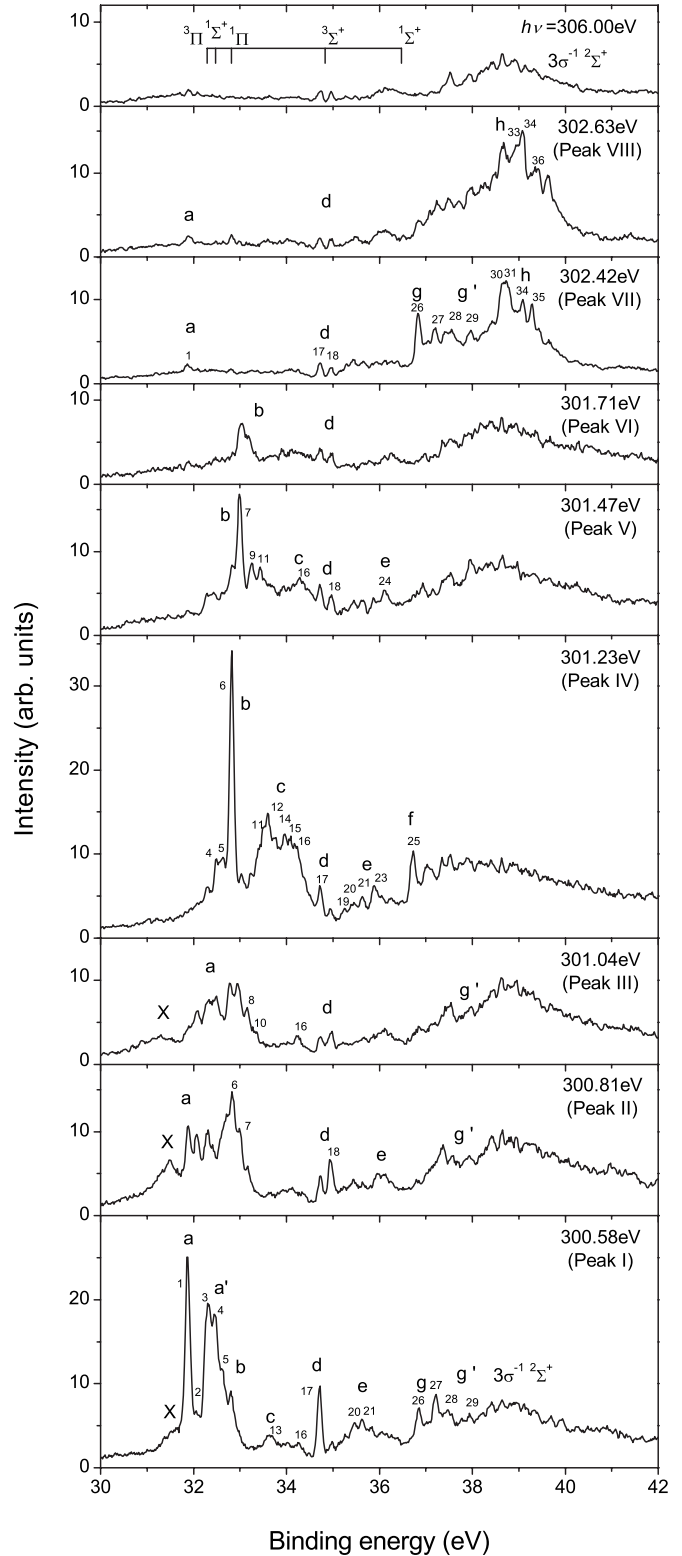


FIG. 3. The angle-independent resonant Auger spectra measured via resonant excitation of the doubly excited Rydberg states labeled peaks I–VIII. For comparison, the photoelectron spectrum measured on top of the  $\sigma^*$  shape resonance ( $h\nu=306$  eV) is also shown. The vertical-bar diagram in the uppermost panel indicates the energy splitting of the  $2h$  parent states. The energy position of the prominent line 6, i.e., the state  $1\pi^{-1}5\sigma^{-1}({}^1\Pi)3s\sigma$  ( ${}^2\Pi$ ) ( $\nu''=0$ ), has been taken as the reference value.

TABLE I. Energy positions and assignments of lines observed in resonant Auger spectra of the doubly excited Rydberg states. The “?” indicates a tentative assignment.

Line	Group	Assignment	Energy (eV)			
			Present work	PES (Ref. [35])	PES (Ref. [15])	TPES Ref. [38]
1	<i>a</i>	$5\sigma^{-2}(^1\Sigma^+)3s(v''=0)$	31.87	31.9	31.88	31.875
2	<i>a</i>	$5\sigma^{-2}(^1\Sigma^+)3s(v''=1)$	32.08	32.08		32.11
3	<i>a'</i>	$1\pi^{-1}5\sigma^{-1}(^3\Pi)3s(v''=0)$	32.32			
4	<i>a'</i>	$1\pi^{-1}5\sigma^{-1}(^3\Pi)3s(v''=1)$	32.48			32.48
5	<i>a'</i>	$1\pi^{-1}5\sigma^{-1}(^3\Pi)3s(v''=2)$	32.64			32.61
6	<i>b</i>	$1\pi^{-1}5\sigma^{-1}(^1\Pi)3s(v''=0)$	32.82	32.826,32.853	32.82	32.820
7	<i>b</i>	$1\pi^{-1}5\sigma^{-1}(^1\Pi)3s(v''=1)$	33.00	32.988,33.045	32.99	32.984
8	<i>b</i>	$1\pi^{-1}5\sigma^{-1}(^1\Pi)3s(v''=2)$	33.16	33.176,33.226	33.17	33.170
9	<i>c</i>	$1\pi^{-1}5\sigma^{-1}(^1\Pi)3s?$	33.24			
10	<i>c</i>	$1\pi^{-1}5\sigma^{-1}(^1\Pi)3s?$	33.32			33.358
11	<i>c</i>	$1\pi^{-1}5\sigma^{-1}(^1\Pi)3s?$	33.43			
12	<i>c</i>	$1\pi^{-1}5\sigma^{-1}(^1\Pi)3s?$	33.64			33.64
13	<i>c</i>	$1\pi^{-1}5\sigma^{-1}(^1\Pi)3s?$	33.68			33.64
14	<i>c</i>	$1\pi^{-1}5\sigma^{-1}(^1\Pi)3s?$	33.93		33.91	33.917
15	<i>c</i>	$1\pi^{-1}5\sigma^{-1}(^1\Pi)3s?$	34.08		34.08	34.087
16	<i>c</i>	$1\pi^{-1}5\sigma^{-1}(^1\Pi)3s?$	34.25		34.24	34.256
17	<i>d</i>	$4\sigma^{-1}5\sigma^{-1}(^3\Sigma^+)3s(v''=0)$	34.72	34.722	34.715	34.712
18	<i>d</i>	$4\sigma^{-1}5\sigma^{-1}(^3\Sigma^+)3s(v''=1)$	34.95	34.962	34.955	34.960
19	<i>e</i>	$4\sigma^{-1}5\sigma^{-1}(^1\Sigma^+)3s$	35.23	35.254	35.245	35.247
20	<i>e</i>	$4\sigma^{-1}5\sigma^{-1}(^1\Sigma^+)3s$	35.44	35.476	35.475	35.48
21	<i>e</i>	$4\sigma^{-1}5\sigma^{-1}(^1\Sigma^+)3s$	35.64		35.66	35.62
22	<i>e</i>	$4\sigma^{-1}5\sigma^{-1}(^1\Sigma^+)3s$	35.77	35.79		35.81
23	<i>e</i>	$4\sigma^{-1}5\sigma^{-1}(^1\Sigma^+)3s$	35.92		35.96	35.98
24	<i>e</i>	$4\sigma^{-1}5\sigma^{-1}(^1\Sigma^+)3s$	36.10	36.113,36.159	36.11	36.110
25	<i>f</i>	$4s?$	36.71		36.72	36.71
26	<i>g</i>	$5\sigma^{-2}(^1\Sigma^+)4s(v''=0)$	36.84		36.85	36.85
27	<i>g</i>	$4s?$	37.22			
28	<i>g'</i>	$4s?$	37.50	37.58	37.53	37.51
29	<i>g'</i>	$4s?$	37.94	37.98	37.95	37.95
30	<i>h</i>	$5\sigma^{-2}(^1\Sigma^+)5s(v''=0)$	38.63	38.68	38.62	38.61
31	<i>h</i>	$5s?$	38.75			

TABLE I. (*Continued.*)

Line	Group	Assignment	Energy (eV)			
			Present work	PES (Ref. [35])	PES (Ref. [15])	TPES Ref. [38]
32	<i>h</i>	$5\sigma^{-2}(^1\Sigma^+)5s(v''=0)$	38.84			
33	<i>h</i>	$5s?$	38.94	38.98	38.94	38.94
34	<i>h</i>	$5s?$	39.08		39.09	39.08
35	<i>h</i>	$5s?$	39.28		39.28	39.27
36	<i>h</i>	$5s?$	39.37		39.37	

### B. Assignment of groups *a* and *a'*

The group *a* consists of lines 1 and 2 while *a'* consists of lines 3–5. These groups are most strongly enhanced in the Auger decay of transition A, i.e., peaks I–III of the ion-yield spectra. In the resonant Auger spectrum of peak I the most intense line is at 31.87 eV. It is also observed in high-resolution inner valence [15,35] and threshold photoelectron [38] spectra. Using higher excitation energies (peak II and higher) the intensity of this line decreases. The resonant Auger spectra of Sundin *et al.* [21] clearly show that the energy position of this line coincides with the onset of the C  $1s^{-1}3s$  ( $v'=0$ ) resonant Auger decay. As Öhrwall *et al.* pointed out this clearly suggests to assign line 1 at 31.87 eV to  $5\sigma^{-2}(^1\Sigma^+)3s\sigma(^2\Sigma^+)$  ( $v''=0$ ); this is in full agreement with the present assignment of transition A to C  $1s^{-1}(5\sigma^{-1}2\pi^1S=1)3s\sigma$ .

The weak line 2 at 32.08 eV has little intensity at peak I, but increases at peaks II and III. There is a corresponding decrease in the intensity of line 1 at 31.87 eV. The  $\approx 210$  meV energy splitting between lines 1 and 2 agrees reasonably well with the vibrational energy of the  $5\sigma^{-2}(^1\Sigma^+)$  parent state [37] leading us to assign line 2 to the  $5\sigma^{-2}(^1\Sigma^+)3s\sigma(^2\Sigma^+)$  ( $v''=1$ ) state. The intensity variation as a function of the excitation energy can be attributed to the change of the intensity distribution of the vibrational substates in the Auger final state as the photon energy is scanned to higher vibrational levels in the core-excited state.

Several overlapping lines that are possibly vibrational substates of the same electronic state are labeled as group *a'* lying slightly above group *a*. An assignment of these lines to vibrational substates is supported by the  $\approx 160$  meV separation between lines 3 and 4, and between lines 4 and 5. In the following we discuss two possible assignments for group *a'*.

A band in the corresponding energy region can be found in the C  $1s^{-1}3s\sigma$  ( $v'=1$ ) resonant Auger spectrum (it is labeled as *b* in Fig. 2 of Ref. [21]). Sundin *et al.* assigned this band as the higher vibronic members of group *a*, i.e., the  $5\sigma^{-2}(^1\Sigma^+)3s\sigma(^2\Sigma^+)$  state, and identified the possible overlap with other electronic final states [21]. Clearly the  $1\pi^{-1}5\sigma^{-1}(^1\Pi)3s\sigma(^2\Pi)$  state (group *b* in Fig. 3) overlaps with group *a'*. The intense band just below 33 eV, which is seen in the spectra obtained at peaks II and III seems to belong to group *a'*. It is possible to assign all peaks in Fig. 3,

which are labeled *a* or *a'*, to vibrational levels of the  $5\sigma^{-2}(^1\Sigma^+)3s\sigma(^2\Sigma^+)$  final state. This series does not have regular energy spacings between vibrational substates, and the vibrational intensity distribution is not Franck-Condon-type. In this context the relatively low intensity of line 2 is particularly atypical of a Franck-Condon-type behavior. Assignment of group *a* and *a'* as vibrational levels of the  $5\sigma^{-2}(^1\Sigma^+)3s\sigma(^2\Sigma^+)$  state suggests a significant interaction with another electronic state.

An alternative assignment of group *a'* can be obtained by considering lines 3–5 separately. In this case the energy splitting of  $\approx 160$  meV agrees well with the  $1\pi^{-1}5\sigma^{-1}(^3\Pi)$  parent state. In addition, the intensities of lines 3–5 in the resonant Auger spectrum of peak I follow a typical Franck-Condon-type vibrational progression. Moreover, line 3 is 500 meV lower in energy than line 6, which is assigned to  $1\pi^{-1}5\sigma^{-1}(^1\Pi)3s\sigma(^2\Pi)$ . This splitting agrees perfectly with the energy difference between the  $1\pi^{-1}5\sigma^{-1}(^3\Pi)$  and  $1\pi^{-1}5\sigma^{-1}(^1\Pi)$  parent states. Based on these arguments the group *a'* can also be assigned to the  $1\pi^{-1}5\sigma^{-1}(^1\Pi)3s\sigma(^2\Pi)$  ( $v''=0,1,2$ ) state.

This state is expected to be populated in the resonant Auger decay of the C  $1s^{-1}5\sigma^{-1}2\pi^13s\sigma$  state, but not in the decay of the C  $1s^{-1}3s\sigma$  state. As a consequence of this assignment, the observed group *a'* is either different from the band observed by Sundin *et al.* in the same energy region of the resonant Auger spectrum of the singly excited state [21] or the additional  $3s\sigma$  Rydberg electron in the C  $1s^{-1}3s\sigma$  state leads to a significant modification of the C  $1s^{-1}\rightarrow 1\pi^{-1}5\sigma^{-1}(^3\Pi)$  Auger intensity. With this assignment the energy differences between the  $1\pi^{-1}5\sigma^{-1}(^3\Pi)3s\sigma(^2\Pi)$ ,  $1\pi^{-1}5\sigma^{-1}(^1\Pi)3s\sigma(^2\Pi)$ ,  $4\sigma^{-1}5\sigma^{-1}(^3\Sigma)3s\sigma(^2\Sigma)$ , and  $4\sigma^{-1}5\sigma^{-1}(^1\Sigma)3s\sigma(^2\Sigma)$  states match the corresponding parent states (see also below), while the  $5\sigma^{-2}(^1\Sigma^+)3s\sigma(^2\Sigma^+)$  is shifted lower in energy relative to its parent state by  $\approx 600$  meV.

In summary, we present two possible assignments for group *a'*. Nevertheless, we tentatively assign this group to the  $1\pi^{-1}5\sigma^{-1}(^3\Pi)3s\sigma(^2\Pi)$  final state since it can be motivated by simple arguments such as vibrational energies and energy positions relative to other states. However, for a more conclusive assignment further studies such as measurements of high-resolution resonant Auger spectra of the C  $1s^{-1}3s\sigma$  excitation or calculations of the potential energy curves of the  $2h-1e$  states are required.

### C. Assignment of group *b*

Group *b* is most intense at peaks IV–VI. The spectrum obtained at peak IV shows a very strong enhancement of line 6 at 32.82 eV. This line is the lowest vibrational substate in group *b* and it has also been observed in the high-resolution inner-valence photoelectron spectra [15,35] as well as the threshold photoelectron spectrum [38]. Line 7 at 33.00 eV reaches its maximum intensity at peaks V and VI and the spectrum obtained at peak VI line 8 at 33.20 eV is also enhanced. These lines are also visible in the direct photoelectron spectra. Peaks of group *b* are only weakly populated at the photon energies of peaks I, VII, and VIII. It is possible that the peaks in group *b* could be populated in the spectra measured at peaks II and III; it is difficult to distinguish them from group *a* since they are not as distinct, and they overlap with group *a*. In the He II  $\beta$  measurement by Baltzer *et al.*, these lines were revealed to be doublets with a 30–50 meV splitting and they assigned them to a state of  $\Pi$  symmetry [35]. Subsequent experiments by Öhrwall *et al.* [15] and Hikosaka *et al.* [38] were not able to resolve the doublet structure, as is the case in the present measurements. Referring to the different dissociation character of these states, Hikosaka *et al.* attributed the lines at 32.98 and 33.17 eV, together with two more lines at 33.36 eV and 33.56 eV, to a vibrational progression of an electronic state different from the first line at 32.82 eV. Baltzer *et al.* attributed these three peaks to one state [35].

We assign these three lines to  $1\pi^{-1}5\sigma^{-1}$  ( $^1\Pi$ )  $3s\sigma$  ( $^2\Pi$ ) with  $v''=0, 1, 2$ . An assignment to a  $2h-1e$  final state with a  $3p$  Rydberg electron can be excluded since the resonant Auger spectrum of the C  $1s^{-1}3p$  excitation shows an onset at 33.5 eV [18], i.e., at higher kinetic energies. In addition, the observed energy spacing between lines 6, 7, and 8 matches the vibrational energies of the  $1\pi^{-1}5\sigma^{-1}$  ( $^1\Pi$ ) parent state. This assignment leads to a splitting of 950 meV between the states  $5\sigma^{-2}$  ( $^1\Sigma^+$ )  $3s\sigma$  ( $^2\Sigma^+$ ) ( $v''=0$ ) and  $1\pi^{-1}5\sigma^{-1}$  ( $^1\Pi$ )  $3s\sigma$  ( $^2\Pi$ ) ( $v''=0$ ). This splitting is still in reasonable agreement with the splitting of 350 meV observed for the parent states. As mentioned above this also results in a splitting between the states  $1\pi^{-1}5\sigma^{-1}$  ( $^3\Pi$ )  $3s\sigma$  ( $^2\Pi$ ) ( $v''=0$ ) and  $1\pi^{-1}5\sigma^{-1}$  ( $^1\Pi$ )  $3s\sigma$  ( $^2\Pi$ ) ( $v''=0$ ) that matches very well with those of the parent states. This assignment is in line with the observed splitting by Baltzer *et al.* and supports further the assignment of the transition *B* in the spectrum of the doubly excited states to C  $1s^{-1}5\sigma^{-1}2\pi^13s\sigma$ . This assignment implies that group *b* should, in principle, be present in the C  $1s^{-1}3s\sigma$  resonant Auger spectra. The only published spectrum, by Sundin *et al.* [21], shows a feature at this energy, but is not able to resolve any lines.

Using the assignments of peaks IV–VI to C  $1s^{-1}$  ( $5\sigma^{-1}2\pi^1S=0$ )  $3s\sigma$  ( $v'=0, 1, 2$ ) and the lines of group *b* to  $1\pi^{-1}5\sigma^{-1}$  ( $^1\Pi$ )  $3s\sigma$  ( $^2\Pi$ ) ( $v''=0, 1, 2$ ) we observe that the most prominent vibrational transitions are  $v'=0 \rightarrow v''=0$ ,  $v'=1 \rightarrow v''=1$ , and  $v'=2 \rightarrow v''=1, 2$ . This is typical for the case where the potential energy curves of the intermediate doubly excited state and the final ionic state have nearly identical equilibrium distances. The equilibrium distance of the doubly excited Rydberg state *B* according to the previous discussion is specified to be 1.174 Å [2]. This value should be

compared to that of the  $1\pi^{-1}5\sigma^{-1}$  ( $^1\Pi$ ) parent state of 1.240 Å [37], suggesting that the  $1\pi^{-1}5\sigma^{-1}$  ( $^1\Pi$ )  $3s\sigma$  ( $^2\Pi$ ) has a smaller equilibrium distance because of the partial valence character of the  $3s\sigma$  orbital.

### D. Assignment of group *c*

The group labeled *c* consists of many unresolved lines in the energy range between 33 and 34.5 eV. As for group *b*, the lines of group *c* are mostly enhanced at peaks IV–VI. The lines overlap substantially making resolution of individual lines impossible. Therefore only the strongest, most well-resolved lines are identified in Table I. Many of these lines coincide with the lines observed in the high-resolution inner-valence photoelectron spectra [15,35] and the threshold photoelectron spectrum [38]. The C  $1s^{-1}3s$  resonant Auger spectrum by Sundin *et al.* [21] also shows some trace of this band. Öhrwall *et al.* assigned these lines to the  $1\pi^{-1}5\sigma^{-1}$  ( $^1\Pi$ )  $3s$  ( $^2\Pi$ ) state.

Using the simple picture of single electron configurations we also expect that the narrow lines in this energy region originate from vibrational substates of the  $1\pi^{-1}5\sigma^{-1}$  ( $^1\Pi$ )  $3s\sigma$  ( $^2\Pi$ ) configuration. However, the energy separations and intensities of these lines do not follow a regular progression as expected for vibrational series. This suggests that configuration interaction may play an important role in this part of the spectrum.

### E. Assignment of groups *d* and *e*

The lines labeled as group *d* at 34.72 and 34.95 eV are observed in the spectra obtained at excitation energies of peaks I–VIII and also in the “background” spectrum at 306 eV. A significant enhancement of these lines is observed only at peaks I–III. Group *d* shows a behavior similar to group *a* concerning the intensity, namely, that the higher-energy peak increases with increasing photon energy (see peaks II and III). The group is visible in the inner-valence photoelectron spectra of Öhrwall *et al.* and Baltzer *et al.* [15,35]. In addition, Hikosaka *et al.* observed these lines in their threshold photoelectron spectrum and assigned them to Rydberg states converging to the  $4\sigma^{-1}5\sigma^{-1}$  ( $^3\Sigma$ ) ionization threshold of CO $^{2+}$  [38]. Although these lines are weak in the C  $1s^{-1}3s$  resonant Auger spectra of Sundin *et al.* [21], we nevertheless assign these lines to  $4\sigma^{-1}5\sigma^{-1}$  ( $^3\Sigma$ )  $3s\sigma$  ( $^2\Sigma$ ) with  $v''=0$  and  $v''=1$  following Hikosaka *et al.* This assignment leads to an energy difference between the  $1\pi^{-1}5\sigma^{-1}$  ( $^1\Pi$ )  $3s\sigma$  ( $^2\Pi$ ) ( $v''=0$ ) and  $4\sigma^{-1}5\sigma^{-1}$  ( $^3\Sigma^+$ )  $3s\sigma$  ( $^2\Sigma^+$ ) ( $v''=0$ ) states of 1.90 eV. This is in agreement with the 2.10 eV splitting of the parent states. In addition, the vibrational splitting of  $\approx 240$  meV also agrees well with the  $\approx 248$  meV value of the parent states [37].

The lines in group *e* are observed in the energy region at  $\approx 36$  eV. It shows a number of lines with irregular spacing. In the C  $1s^{-1}3s$  resonant Auger spectra, Sundin *et al.* found a strong enhancement in this energy region and assigned the corresponding lines to the vibrational components of the  $4\sigma^{-1}5\sigma^{-1}$  ( $^1\Sigma^+$ )  $3s\sigma$  ( $^2\Sigma^+$ ). As can be seen from the diagram in the uppermost panel of Fig. 3 indicating the splittings of the parent states, this assignment agrees well with the ex-

pected energy position for this final state. The irregular spacing can be accounted for by assignment to vibrational sub-states since the  $4\sigma^{-1}5\sigma^{-1} ({}^1\Sigma^+)$  parent state possesses a double-well potential with the maximum of the barrier close to the Franck-Condon region of the resonant Auger decay [37]. Such a potential can readily explain both the irregular peak separations, and the intensities of the peaks. In addition, a partial valence character of the  $3s\sigma$  Rydberg electron might in this particular case lead to a strong modification of the potential shape, such as, e.g., a vanishing of the double-well structure of the potential. This would lead to a further modification of the vibrational progression.

#### F. Assignment of the groups $f$ , $g$ , $g'$ , and $h$

In the higher-energy region the groups  $f$ ,  $g$ ,  $g'$ , and  $h$  are visible. Based on the energies of the parent states and the Rydberg formula, one can determine the principal quantum number  $n$  of the Rydberg electron. Thus we assign the groups  $f$ ,  $g$ , and  $g'$  to one of the final states  $1\pi^{-1}5\sigma^{-1} ({}^3\Pi) 4s\sigma ({}^2\Pi)$ ,  $5\sigma^{-2} ({}^1\Sigma^+) 4s\sigma ({}^2\Sigma^+)$ , and  $1\pi^{-1}5\sigma^{-1} ({}^1\Pi) 4s\sigma ({}^2\Pi)$  and those of group  $h$  to the final states  $1\pi^{-1}5\sigma^{-1} ({}^3\Pi) 5s\sigma ({}^2\Pi)$ ,  $5\sigma^{-2} ({}^1\Sigma^+) 5s\sigma ({}^2\Sigma^+)$ , and  $1\pi^{-1}5\sigma^{-1} ({}^1\Pi) 5s\sigma ({}^2\Pi)$  states. However, a more detailed and conclusive assignment is not possible since (i) the sequence of the energy positions of the  $1\pi^{-1}5\sigma^{-1} ({}^3\Pi) 3s\sigma ({}^2\Pi)$ ,  $5\sigma^{-2} ({}^1\Sigma^+) 3s\sigma ({}^2\Sigma^+)$ ,  $1\pi^{-1}5\sigma^{-1} ({}^1\Pi) 3s\sigma ({}^2\Pi)$  states differs from that of the parent states (see above) and (ii) the groups  $f$ ,  $f'$ ,  $g$ , and  $h$  are partially visible in the inner-valence photoelectron spectrum, i.e., they interact with the  $3\sigma^{-1} ({}^2\Sigma^+)$  final state. Due to these arguments we assume that the energy positions of the  $ns$  Rydberg states do not strictly follow the Rydberg formula, i.e., the Rydberg formula is not suitable for determination of the limit of this  $ns$  Rydberg series.

Our tentative assignments of the individual groups  $f$ ,  $g$ , and  $g'$  and their reasoning are as follows. The lines of group  $g$  are visible in the Auger spectra of the resonantly enhanced states  $C 1s^{-1} (5\sigma^{-1}2\pi^1 S=1) 3s\sigma$  and  $C 1s^{-1} (5\sigma^{-1}2\pi^1 S=1) 4s\sigma$ , i.e., peaks I–III and VII and VIII, respectively. By assuming that the Rydberg electron does not significantly influence the Auger transition rates and the equilibrium distances of the final states we tentatively assign group  $g$  to  $5\sigma^{-2} ({}^1\Sigma^+) 4s\sigma ({}^2\Sigma^+)$ . This assignment is based on the fact that the behavior of the strong individual line 26 at 36.84 eV in the decay of the excitation  $C 1s^{-1} (5\sigma^{-1}2\pi^1 S=1) 4s\sigma (v'=0)$  resembles the behavior of the line 1 in the Auger spectrum of the  $C 1s^{-1} (5\sigma^{-1}2\pi^1 S=1) 3s\sigma (v'=0)$  excitation.

By assuming that the presence of groups  $f$ ,  $g$ , and  $g'$  in the resonant Auger spectra measured at peaks I–VI are due to a  $3s \rightarrow 4s$  shake up and by assuming that the intensity of the different  $4s$  states follows the intensities of the  $2h-1e$  final states with a  $3s$  Rydberg electron we assign  $1\pi^{-1}5\sigma^{-1} ({}^1\Pi) 4s\sigma ({}^2\Pi)$  to group  $f$ ,  $5\sigma^{-2} ({}^1\Sigma^+) 4s\sigma ({}^2\Sigma^+)$  to group  $g$ , and  $1\pi^{-1}5\sigma^{-1} ({}^3\Pi) 4s\sigma ({}^2\Pi)$  to group  $g'$ . However, this assignment is—at least for  $f$  and  $g'$ —not at all conclusive since the energy ordering of the final states differs from both the parent states and the final states with an additional  $3s$  Rydberg electron. This clearly shows the limits for an assignment of

the higher- $n$  Rydberg states based on simple arguments.

As mentioned above the final states of group  $h$  are  $1\pi^{-1}5\sigma^{-1} ({}^3\Pi) 5s\sigma ({}^2\Pi)$ ,  $5\sigma^{-2} ({}^1\Sigma^+) 5s\sigma ({}^2\Sigma^+)$ , and  $1\pi^{-1}5\sigma^{-1} ({}^1\Pi) 5s\sigma ({}^2\Pi)$  arising from a  $4s \rightarrow 5s$  shake-up transition. The separation between lines 30 and 32 at 38.63 and 38.84 eV matches the vibrational spacing of the  $5\sigma^{-2} ({}^1\Sigma^+)$  parent state so that we assign these lines to  $5\sigma^{-2} ({}^1\Sigma^+) 5s\sigma ({}^2\Sigma^+)$  ( $v''=0, 1$ ). For all other lines of this group no clear assignment can be given.

#### G. Assignment of the broad feature X

Line X at 31.5 eV is a broad, featureless structure implying a weakly bound or dissociative final state. This line is only observed in the resonant Auger spectra at peaks I–III, i.e., the  $C 1s^{-1}5\sigma^{-1}2\pi^1 (S=1) 3s\sigma$  excitation. Since these peaks overlap with the  $C 1s^{-1}1\pi^{-1}2\pi^1 3s\sigma$  state (see  $0^\circ$  spectrum in Fig. 2) it is also possible that the enhancement is due to decay of the latter state.

Eland *et al.* [36] calculated the potential curves of the parent states and found the dissociative state  $1\pi^{-2} ({}^3\Sigma^-)$  with a very small hump at bond distances between 1.5 and 2 Å in the energy region just below the  $1\pi^{-1}5\sigma^{-1} ({}^1\Pi)$  and  $5\sigma^{-2} ({}^1\Sigma^+)$  parent states. Based on its energy position relative to the  $1\pi^{-1}5\sigma^{-1} ({}^3\Pi) 3s\sigma ({}^2\Pi)$  and  $5\sigma^{-2} ({}^1\Sigma^+) 3s\sigma ({}^2\Sigma^+)$  states we assign feature X to a  $1\pi^{-2} ({}^1\Sigma^+) 3s\sigma ({}^2\Sigma^-)$  state. The potential energy curve and the partial valence character of the  $3s\sigma$  electron suggest a weakly bound state with unresolved vibrational structure. A transition to the corresponding parent state ( ${}^3\Sigma^-$ ) was not observed in the normal Auger spectrum due to its triplet character [37]. However, for doubly excited states the first hole in the  $1\pi$  orbital is created by the excitation process so that the Auger decay to the  $1\pi^{-2} ({}^3\Sigma^-)$  parent state is due to an interplay of a  $1\pi$  and the  $2\pi$  electron but not between two  $1\pi$  electrons. Thus the transition rate to this final state can differ considerably from that in the normal Auger spectrum.

#### V. CONCLUSIONS

The doubly excited states of carbon monoxide in the photon energy region of 300–305 eV have been studied with angle-resolved ion-yield spectroscopy and high-resolution resonant Auger spectroscopy. Symmetry-resolved ion-yield spectra identify the doubly excited Rydberg states at  $\approx 300$  eV to be of  $\Pi$  character. The leading configurations for the doubly excited Rydberg states are derived by using a simple model to compare states with similar configurations, and are confirmed by the analysis of the corresponding resonant Auger spectra. The analysis suggests that state A in the ion-yield spectrum is the  $C 1s^{-1}5\sigma^{-1}2\pi^1 (S=1) 3s\sigma$  with vibrational substates. The leading configuration of the second state (transition B) is the  $C 1s^{-1}5\sigma^{-1}2\pi^1 (S=0) 3s\sigma$  and that of the third transition (transition C) is the  $C 1s^{-1}5\sigma^{-1}2\pi^1 (S=1) 4s\sigma$  configuration, both with clear vibrational substates. The excitation of these states can be explained by a conjugate shake-up process with a  $C 1s^{-1} \rightarrow 1\pi$  excitation accompanied by a  $5\sigma \rightarrow ns\sigma$  shake transition. From the resonant Auger spectra we assign a large number of the  $2h-1e$

final states which are also present in published inner-valence photoelectron spectra. The assignment of the  $2h-1e$  final states is, however, in some cases ambiguous since the experimental findings are not entirely in line with the implications of the Rydberg formula or the splitting of the parent states.

Combining symmetry-resolved ion-yield studies with angle-resolved resonant Auger spectroscopy provides deeper insight into the origins of both the core-excited states, and of the final two-hole one-electron states. In this study we are able to unravel complex overlapping states and identify a large number of configurations in the spectra. Some ambiguities remain, especially with respect to the assignment of the final states. For the states which are not easily assigned, resonant Auger studies of the  $C\ 1s^{-1}3s\sigma$  excitation could contribute to an understanding of the origin of additional lines. The medium-resolution resonant Auger spectrum of this excitation presented by Sundin *et al.* [21] matches, however, quite well the overall shape of the high-resolution normal Auger spectra recorded subsequent to  $C\ 1s$  ionization [37] so that strongly overlapping vibrational progressions are expected in

high-resolution spectra. In contrast to  $C\ 1s$  ionization the vibrational progressions in the normal Auger spectra subsequent to  $O\ 1s$  ionization are much shorter [37]. Since this probably also holds for the resonant Auger spectra of the  $O\ 1s^{-1}3s\sigma$  excitation an assignment of the final states based on these spectra might be much easier. In addition, accurate calculation of the potential-energy curves for final states will certainly aid in assignment.

#### ACKNOWLEDGMENTS

This experiment was carried out with the approval of the SPring-8 program review committee and supported in part by Grants-in-Aid for Scientific Research from the Japan Society for the Promotion of Science (JSPS). R.P. and T.T. acknowledge JSPS for financial support. R.P. also acknowledges Tohoku University for support and hospitality during his stay at Tohoku University. The Swedish Research Council is acknowledged for financial support by S.L.S.

- 
- [1] J.-I. Adachi, N. Kosugi, and A. Yagishita, *J. Phys. B* **38**, R127 (2005).
- [2] M. Domke, C. Xue, A. Pushmann, T. Mandel, E. Hudson, D. A. Shirley, and G. Kaindl, *Chem. Phys. Lett.* **173**, 122 (1990); **174**, 668 (1990).
- [3] A. P. Hitchcock and C. E. Brion, *J. Electron Spectrosc. Relat. Phenom.* **18**, 1 (1980).
- [4] D. A. Shaw, G. C. King, D. Cvejanović, and F. H. Read, *J. Phys. B* **17**, 2091 (1984).
- [5] Y. Ma, C. T. Chen, G. Meigs, K. Randall, and F. Sette, *Phys. Rev. A* **44**, 1848 (1991).
- [6] E. Shigemasa, T. Hayaishi, T. Sasaki, and A. Yagishita, *Phys. Rev. A* **47**, 1824 (1993).
- [7] P. Erman, A. Karawajczyk, E. Rachlew-Källne, and C. Strömholm, *J. Phys. B* **28**, 2069 (1995).
- [8] H. M. Köppe, A. L. D. Kilcoyne, J. Feldhaus, and A. M. Bradshaw, *J. Electron Spectrosc. Relat. Phenom.* **75**, 97 (1995).
- [9] H. M. Köppe, B. Kempgens, A. L. D. Kilcoyne, J. Feldhaus, and A. M. Bradshaw, *Chem. Phys. Lett.* **260**, 223 (1996).
- [10] W. C. Stolte, D. L. Hansen, M. N. Piancastelli, I. Dominguez Lopez, A. Rizvi, O. Hemmers, H. Wang, A. S. Schlachter, M. S. Lubell, and D. W. Lindle, *Phys. Rev. Lett.* **86**, 4504 (2001).
- [11] H. Ågren and R. Arneberg, *Phys. Scr.* **30**, 55 (1984).
- [12] K. Ueda, *J. Phys. B* **36**, R1 (2003).
- [13] S. Svensson, *J. Phys. B* **38**, S821 (2005).
- [14] K. Ueda, *J. Phys. Soc. Jpn.* **75**, 032001 (2006).
- [15] G. Öhrwall, S. Sundin, P. Baltzer, and J. Bozek, *J. Phys. B* **32**, 463 (1999).
- [16] M. Schmidbauer, A. L. D. Kilcoyne, H.-M. Köppe, J. Feldhaus, and A. M. Bradshaw, *Phys. Rev. A* **52**, 2095 (1995).
- [17] M. Schmidbauer, A. L. D. Kilcoyne, H.-M. Köppe, J. Feldhaus, and A. M. Bradshaw, *Chem. Phys. Lett.* **199**, 119 (1992).
- [18] S. Sundin, S. J. Osborne, A. Ausmees, O. Björneholm, S. L. Sorensen, A. Kikas, and S. Svensson, *Phys. Rev. A* **56**, 480 (1997).
- [19] S. Sundin, F. Kh. Gel'mukhanov, S. J. Osborne, O. Björneholm, A. Ausmees, A. Kikas, S. L. Sorensen, A. Naves de Brito, R. R. T. Marinho, S. Svensson, and H. Ågren, *J. Phys. B* **30**, 4267 (1997).
- [20] M. N. Piancastelli, M. Neeb, A. Kivimäki, B. Kempgens, H. M. Köppe, K. Maier, A. M. Bradshaw, and R. F. Fink, *J. Phys. B* **30**, 5677 (1997).
- [21] S. Sundin, S. L. Sorensen, A. Ausmees, O. Björneholm, I. Hjelte, A. Kikas, S. Svensson, and H. Ågren, *J. Phys. B* **32**, 267 (1999).
- [22] O. Hemmers, F. Heiser, J. Vieffhaus, K. Wieliczek, and U. Becker, *J. Phys. B* **32**, 3769 (1999).
- [23] E. Kukk, J. D. Bozek, W.-T. Cheng, R. F. Fink, A. A. Wills, and N. Berrah, *J. Chem. Phys.* **111**, 9642 (1999).
- [24] H. Ohashi, E. Ishiguro, Y. Tamenori, H. Kishimoto, M. Tanaka, M. Irie, T. Tanaka, and T. Ishikawa, *Nucl. Instrum. Methods Phys. Res. A* **467-468**, 529 (2001).
- [25] H. Ohashi, E. Ishiguro, Y. Tamenori, H. Okumura, A. Hiraya, H. Yoshida, Y. Senba, K. Okada, N. Saito, I. H. Suzuki, K. Ueda, T. Ibuki, S. Nagaoka, I. Koyano, and T. Ishikawa, *Nucl. Instrum. Methods Phys. Res. A* **467-468**, 533 (2001).
- [26] Y. Tamenori, H. Ohashi, E. Ishiguro, and T. Ishikawa, *Rev. Sci. Instrum.* **73**, 1588 (2002).
- [27] Y. Shimizu, H. Yoshida, K. Okada, Y. Muramatsu, N. Saito, H. Ohashi, Y. Tamenori, S. Fritzsche, N. M. Kabachnik, H. Tanaka, and K. Ueda, *J. Phys. B* **33**, L685 (2000).
- [28] Y. Shimizu, H. Ohashi, Y. Tamenori, Y. Muramatsu, H. Yoshida, K. Okada, N. Saito, H. Tanaka, I. Koyano, S. Shin, and K. Ueda, *J. Electron Spectrosc. Relat. Phenom.* **114-116**, 63 (2001).
- [29] T. Tanaka and H. Kitamura, *J. Synchrotron Radiat.* **3**, 47 (1996).
- [30] N. Saito, K. Ueda, M. Simon, K. Okada, Y. Shimizu, H. Chiba, Y. Senba, H. Okumura, H. Ohashi, Y. Tamenori, S. Nagaoka,

- A. Hiraya, H. Yoshida, E. Ishiguro, T. Ibuki, I. H. Suzuki, and I. Koyano, *Phys. Rev. A* **62**, 042503 (2000).
- [31] C. Pan and H. P. Kelly, *Phys. Rev. A* **39**, 6232 (1989).
- [32] D. W. Lindle, L. J. Medhurst, T. A. Ferrett, P. A. Heimann, M. N. Piancastelli, S. H. Liu, and D. A. Shirley, T. A. Carlson, P. C. Deshmukh, G. Nasreen, and S. T. Manson, *Phys. Rev. A* **38**, 2371 (1988).
- [33] K. Ueda, M. Hoshino, T. Tanaka, M. Kitajima, H. Tanaka, A. De Fanis, Y. Tamenori, M. Ehara, F. Oyagi, K. Kuramoto, and H. Nakatsuji, *Phys. Rev. Lett.* **94**, 243004 (2005).
- [34] S. L. Sorensen, M. Kitajima, T. Tanaka, M. Hoshino, H. Tanaka, Y. Tamenori, R. Sankari, M. N. Piancastelli, K. Ueda, Y. Velkov, I. Minkov, V. Carravetta, and F. Gel'mukhanov, *Phys. Rev. A* **76**, 062704 (2007).
- [35] P. Baltzer, M. Lundqvist, B. Wannberg, L. Karlsson, M. Larsson, M. A. Hayes, J. B. West, M. R. F. Siggel, A. C. Parr, and J. L. Dehmer, *J. Phys. B* **27**, 4915 (1994).
- [36] J. H. D. Eland, M. Hochlaf, G. C. King, P. S. Kreynin, R. J. LeRoy, I. R. McNab, and J.-M. Robbe, *J. Phys. B* **37**, 3197 (2004).
- [37] R. Püttner, X.-J. Liu, H. Fukuzawa, T. Tanaka, M. Hoshino, H. Tanaka, J. Harries, Y. Tamenori, V. Carravetta, and K. Ueda, *Chem. Phys. Lett.* **445**, 6 (2007).
- [38] Y. Hikosaka, M. Ahmad, P. Lablanquie, F. Penent, R. I. Hall, J. H. D. Eland, *J. Electron Spectrosc. Relat. Phenom.* **125**, 99 (2002).